



HAL
open science

New Polydentate Ligand and Catalytic Properties of the Corresponding Ruthenium Complex During Sulfoxidation and Alkene Epoxidation

Olivier Hamelin, Stéphane Ménage, Florence Charnay, Murielle Chavarot, Jean-Louis Pierre, Jacques Pecault, Marc Fontecave

► **To cite this version:**

Olivier Hamelin, Stéphane Ménage, Florence Charnay, Murielle Chavarot, Jean-Louis Pierre, et al.. New Polydentate Ligand and Catalytic Properties of the Corresponding Ruthenium Complex During Sulfoxidation and Alkene Epoxidation. *Inorganic Chemistry*, 2008, 47 (14), pp.6413-6420. 10.1021/ic800534v . hal-01188649

HAL Id: hal-01188649

<https://hal.science/hal-01188649v1>

Submitted on 14 Nov 2023

HAL is a multi-disciplinary open access archive for the deposit and dissemination of scientific research documents, whether they are published or not. The documents may come from teaching and research institutions in France or abroad, or from public or private research centers.

L'archive ouverte pluridisciplinaire **HAL**, est destinée au dépôt et à la diffusion de documents scientifiques de niveau recherche, publiés ou non, émanant des établissements d'enseignement et de recherche français ou étrangers, des laboratoires publics ou privés.

New Polydentate Ligand and Catalytic Properties of the Corresponding Ruthenium Complex During Sulfoxidation and Alkene Epoxidation

Olivier Hamelin,^{*,†} Stéphane Ménage,[†] Florence Charnay,[†] Murielle Chavarot,[†]
Jean-Louis Pierre,[‡] Jacques Pécaut,[§] and Marc Fontecave[†]

Laboratoire de Chimie et Biochimie des Métaux; Université Joseph Fourier, Grenoble, France;
CNRS UMR 5249, France; CEA, DSV/ iRTSV/LCBM, Grenoble, France;
CEA-Grenoble, Bat K, 17 rue des Martyrs, F-38054 Grenoble Cedex 9, Département Chimie Moléculaire;
Université Joseph Fourier, Grenoble, France; CNRS UMR 5250, France; Université Joseph Fourier - Grenoble 1, BP 53,
38041 Grenoble Cedex 9, and Service de Chimie Inorganique et Biologique; Université Joseph Fourier, Grenoble, France;
CEA, DSM/DRFMC/SCIB, CEA-Grenoble, 17 rue des Martyrs, F-38054 Grenoble Cedex 9, France

Bis(diimine)-ruthenium complexes constitute a class of catalysts with good activity for oxidation reactions, such as sulfoxidation and epoxidation. The synthesis and the full characterization of a new ruthenium complex bearing an original pentadentate ligand (L5pyr for 2,6-bis-(6-ethyl-2,2'-bipyridyl)-pyridine) is reported. Comparison of its activity with regard to $[\text{Ru}(\text{bpy})_2(\text{CH}_3\text{CN})_2]^{2+}$ and $[\text{Ru}(\text{bpy})_2(\text{py})(\text{CH}_3\text{CN})]^{2+}$ during alkene and sulfide oxidation allowed us to conclude that the addition of a fifth pyridine ligand in the coordination sphere improves the efficiency of the catalyst. Moreover, under these oxidation conditions a hydroxylation of the ligand L5pyr led to a better activity than its analogue $[\text{Ru}(\text{bpy})_2(\text{py})(\text{CH}_3\text{CN})]^{2+}$, especially during epoxidation of alkenes by $\text{PhI}(\text{OAc})_2$.

Introduction

Ruthenium polypyridyl complexes such as $[\text{Ru}(\text{bpy} \text{ and derivatives})_2\text{XX}']^{2+}$ (bpy = 2,2'-bipyridine, X = X' = CH₃CN or X = Py, X' = O), $[\text{Ru}(\text{dmp})_2(\text{CH}_3\text{CN})_2]^{2+}$, and $[\text{Ru}(\text{tpa} \text{ and derivatives})\text{Cl}_2]$ (tpa = tris(pyridylmethyl)amine) provide an important class of stoichiometric and catalytic oxidants.^{1,2}

Mechanistic studies suggested that in most cases these reactions proceeded via high-valent Ru-oxo intermediate species, which exhibit rich oxidation chemistry.³ Whereas it is becoming increasingly clear that hydrogen atom abstraction is the dominant mechanism for C–H bond oxidation by such

Ru-oxo,⁴ direct oxygen atom transfer to the substrate is likely to occur during epoxidation⁵ and sulfoxidation. In agreement with such a metal-based mechanism, chiral versions of these complexes, with the chirality introduced on the ligands⁶ or at the metal center itself,^{2c} have been recently shown to catalyze the asymmetric oxidation of sulfides and olefins, with reasonable enantioselectivities.

Today, comparison of N₅- with N₄-coordination in terms of the activity and the stability of the corresponding ruthenium complexes has not been directly addressed so far. To do so, we had to synthesize a novel pentadentate bis-diimine N5 ligand, named L5pyr for 2,6-bis-(6-ethyl-2,2'-bipyridyl)-pyridine, in which the two bipyridine moieties are covalently

* To whom correspondence should be addressed. E-mail: ohamelin@cea.fr, Phone: 00(33)438789108.

[†] Laboratoire de Chimie et Biochimie des Métaux; Université Joseph Fourier.

[‡] Département Chimie Moléculaire; Université Joseph Fourier.

[§] Service de Chimie Inorganique et Biologique; Université Joseph Fourier.

(1) Naota, T.; Takaya, H.; Murahashi, S.-I. *Chem. Rev.* **1998**, *98*, 2599.

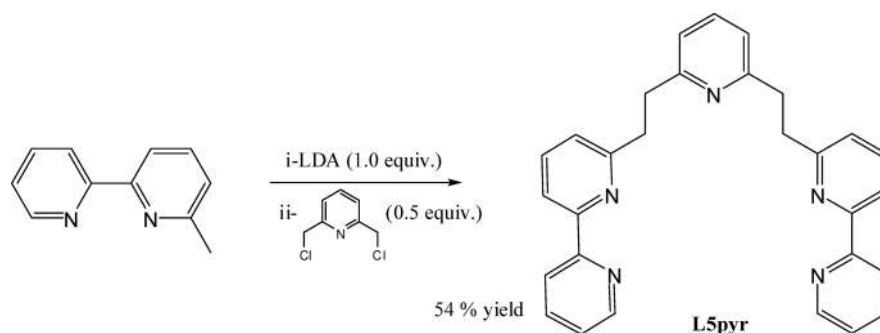
(2) (a) Goldstein, A. S.; Beer, R. H.; Drago, R. S. *J. Am. Chem. Soc.* **1994**, *116*, 2424. (b) Collin, J. P.; Sauvage, J. P. *Inorg. Chem.* **1986**, *25*, 135. (c) Che, C. M.; Li, C. K.; Tang, W. T.; Yu, W. Y. *J. Chem. Soc.; Dalton Trans.* **1992**, 3153. (d) Che, C.-M.; Cheng, K.-W.; Chan, M. C. W.; Lau, T.-C.; Mak, C.-K. *J. Org. Chem.* **2000**, *65*, 7996. (e) Chavarot, M.; Ménage, S.; Hamelin, O.; Charnay, F.; Pécaut, J.; Fontecave, M. *Inorg. Chem.* **2003**, *42*, 4810. (f) Goldstein, A. S.; Drago, R. S. *J. Chem. Soc., Chem. Commun.* **1991**, 21.

(3) (a) Meyer, T. J.; Huynh, M. H. V. *Inorg. Chem.* **2003**, *42*, 8140. (b) Jitsukawa, K.; Oka, Y.; Yamaguchi, S.; Masuda, H. *Inorg. Chem.* **2004**, *43*, 8119. (c) Barf, G. A.; Sheldon, R. A. *J. Mol. Catal., A* **1995**, *102*, 23.

(4) (a) Bryant, J.; Mayer, J. M. *J. Am. Chem. Soc.* **2003**, *125*, 10351. (b) Stultz, L. K.; Huynh, M. V.; Binstead, R. A.; Curry, M.; Meyer, T. J. *J. Am. Chem. Soc.* **2000**, *122*, 5984. (c) Bryant, J. R.; Matsuo, T.; Mayer, J. M. *Inorg. Chem.* **2004**, *43*, 1587.

(5) (a) Scok, W. K.; Meyer, T. J. *J. Am. Chem. Soc.* **1988**, *110*, 7358. (b) Scok, W. K.; Dobson, J. C.; Meyer, T. J. *Inorg. Chem.* **1988**, *27*, 3. (c) Stultz, L. K.; Binstead, R. A.; Reynolds, M. S.; Meyer, T. J. *J. Am. Chem. Soc.* **1995**, *117*, 2520.

(6) Fung, W. H.; Cheng, W. C.; Yu, W. Y.; Che, C. M.; Mak, T. C. W. *J. Chem. Soc., Chem. Commun.* **1995**, 2007.



attached one to the other through a linker containing a pyridinyl group allowing a fifth nitrogen-coordination to the ruthenium center (scheme 1). This compound was used to prepare and characterize the novel ruthenium(II) complex $[\text{Ru}(\text{L5pyr})(\text{CH}_3\text{CN})]^{2+}$ **1**, which can thus be compared to complex $[\text{Ru}(\text{bpy})_2(\text{CH}_3\text{CN})_2]^{2+}$, **2**, and $[\text{Ru}(\text{bpy})_2(\text{py})(\text{CH}_3\text{CN})]^{2+}$, **3**, to evaluate both the importance of the fifth pyridine ligand and the chelating effect on catalysis. A structure–reactivity study has been undertaken with these complexes for sulfide oxidation by H_2O_2 and olefin epoxidation by $\text{PhI}(\text{OAc})_2$ ($\text{OAc} = \text{acetate}$). Here, we demonstrate the importance of the (fifth pyridine) additional pyridine ligand for catalytic activity, as shown from the superiority of catalysts **1** and **3**. Furthermore, with **1** we report a rare case of catalyst self-oxidation, which does not result in an inactivation. Instead, the modified catalyst allows greater reaction yield and is less sensitive than **3** with regard to inhibitors such as acetate.

Experimental Section

Materials. Commercially available chemicals were purchased and used without further purification. $[\text{Ru}(\text{bpy})_2(\text{CH}_3\text{CN})_2][\text{PF}_6]_2$ **2** was prepared according to literature procedure⁶ as for 6-methyl-2,2'-bipyridine.⁹

Physical Measurements. ^1H NMR spectra were recorded on a Bruker DPX 300 at room temperature. Chemical shifts (in ppm) were referenced to the residual protic solvent peaks. ESI-MS Mass Spectrometry was performed on a Finnigan LC-Q instrument. Elemental analyses were performed at the Centrale d'Analyse CNRS (Vernaison, France).

X-ray Crystallography. Data collection was performed at 298 K using a Bruker SMART system equipped with a graphite monochromator $\text{Mo K}\alpha$ ($\lambda = 0.71073 \text{ \AA}$) radiation and a CCD detector. Cell constants were determined from data collections harvested from a set of 20–30 frames. Molecular structures were solved by direct methods and refined on F^2 by full matrix least-squares techniques using *SHELX TL* package with anisotropic thermal parameters. All non-hydrogen atoms were refined anisotropically, and hydrogen atoms were placed in ideal positions and refined as riding atoms with individual isotropic displacement parameters.

Cyclic voltammetry and controlled potential electrolysis experiments were performed using a PAR model 273 potentiostat/galvanostat, a PAR model 175 universal programmer, and a PAR

model 179 digital coulometer. Potentials are referred to an $\text{Ag}/10 \text{ mM AgCl}$ reference electrode in acetone + 0.1 M TBAP. Under these conditions, the redox couple of Fc/Fc^+ was determined at 0.750 V. The working electrodes were platinum and vitreous carbon disks. EPR spectra were recorded with a Bruker ESP 300E at $T = 10 \text{ K}$ using an Oxford 900 cryostat.

Syntheses of Compounds. 2,6-bis(6-ethyl-2,2'-bipyridyl)pyridine (**L5pyr**). To a solution of 500 mg (2.94 mmoles) of 6-methyl-2,2'-bipyridine in anhydrous THF (20 mL) under argon and at $0 \text{ }^\circ\text{C}$, 1.75 mL (2.94 mmoles) of a freshly prepared 1.68 M solution of LDA in THF was added dropwise. The intense purple-blue solution was stirred for 15 min at $0 \text{ }^\circ\text{C}$, and then a solution of 238 mg (1.47 mmoles) of 2,6-bis(chloromethyl)pyridine in anhydrous ether (5 mL) was added dropwise and the solution turned red-brown. The solution was stirred at $0 \text{ }^\circ\text{C}$ for an additional 30 min, then hydrolyzed with a saturated solution of NaHCO_3 , and the organic solvent evaporated under reduce pressure. Extraction of the resulting aqueous solution with dichloromethane, evaporation of the solvent, and purification of the residue on neutral alumina column (30%, 50%, then 70% of ethyl acetate–cyclohexane) afforded 350 mg (0.8 mmole; 54%) of the product as a white solid. Mp 120–122 $^\circ\text{C}$; ^1H NMR (300 MHz, CDCl_3) δ 8.66 (m, 2H), 8.46 (d, $J = 7.89 \text{ Hz}$, 2H), 8.19 (d, $J = 7.72 \text{ Hz}$, 2H), 7.60–7.85 (m, 4H), 7.42 (t, $J = 7.89 \text{ Hz}$, 1H), 7.28 (m, 2H), 7.11 (dd, $J = 7.54, 1.03 \text{ Hz}$, 2H), 6.96 (d, $J = 7.88 \text{ Hz}$, 2H), 3.33 (s, 8H); ^{13}C NMR (76 MHz, CDCl_3) δ 160.7 (C), 160.4 (C), 156.4 (C), 155.3 (C), 148.9 (C), 136.8 (CH), 136.6 (CH), 136.3 (CH), 123.4 (CH), 122.9 (CH), 121.1 (CH), 120.1 (CH), 118.2 (CH), 38.0 (CH_2), 37.7 (CH_2); mass spectrum (FAB+, NBA), m/z (relative intensity) 444 (MH+, 100); Anal. Calcd for $\text{C}_{29}\text{H}_{25}\text{N}_5$: C, 78.53; H, 5.68; N, 15.79. Found C, 78.84; H, 5.45; N, 15.79.

$[\text{Ru}(\text{bpy})_2(\text{py})(\text{CH}_3\text{CN})][\text{PF}_6]_2$ ([3][PF₆]₂**).** To a solution of 30 mg (42.3 μmoles) of $[\text{Ru}(\text{bpy})_2(\text{py})\text{Cl}][\text{PF}_6]^{10}$ in a mixture of acetone–water (6:3 mL), 23.5 mg (94.6 μmoles) of AgPF_6 were added. The resulting suspension was then refluxed for 2 h in the dark. The precipitate was filtered off, and the filtrate was evaporated to dryness in vacuo. The resulting $[\text{Ru}(\text{bpy})_2(\text{py})(\text{H}_2\text{O})][\text{PF}_6]_2$ complex was then dissolved in acetonitrile (1 mL), and the solution was stirred in the dark for 1 h. Precipitation of the complex by addition of the previous solution in a large volume of ether, filtration, and drying in vacuo afforded the complex (31 mg; 85% yield) as an orange powder. Recrystallization by slow diffusion of ether in a solution of the complex in acetone afforded single crystals suitable for X-ray analysis. Pertinent crystallographic data are summarized in Table 1: Triclinic, $p1$, $a = 10.5683 \pm 0.0015$, $b = 12.3778 \pm 0.0017$, $c = 16.646 \pm 0.002 \text{ \AA}$; $V = 1940.3 \pm 0.5 \text{ \AA}^3$; $Z = 4$; $R = 0.0357$.

^1H NMR (300 MHz, CD_3CN (ppm)) 9.40 (ddd, 1H, $J = 0.6, 1.5, 5.7 \text{ Hz}$), 8.55 (d, 1H, $J = 8.1 \text{ Hz}$), 8.47 (ddd, 1H, $J = 0.6, 1.2,$

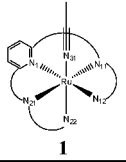
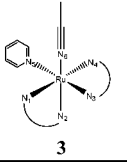
(7) Brown, G. M.; Callahan, R. W.; Meyer, T. J. *Inorg. Chem.* **1975**, *14*, 1915.

(8) Nagao, H.; Hirano, T.; Tsuboya, N.; Hiota, S.; Mukaida, M.; Oi, T.; Yamasaki, M. *Inorg. Chem.* **2003**, *41*, 62467.

(9) Graf, E. *Synthesis* **1992**, 519.

(10) Moyar, B. A.; Meyer, T. J. *Inorg. Chem.* **1981**, *20*, 436.

Table 1. Selected Bond Lengths (Angstroms) and Angles (Degrees) for **1** and **3**^a

			
Ru-N ₁	2.1902(17)	Ru-N ₅	2.107(3)
Ru-N ₁₁	2.0975(17)	Ru-N ₄	2.067(3)
Ru-N ₁₂	2.0447(18)	Ru-N ₃	2.058(3)
Ru-N ₂₁	2.1205(16)	Ru-N ₁	2.057(2)
Ru-N ₂₂	2.0630(16)	Ru-N ₂	2.055(2)
Ru-N ₃₁	2.0431(18)	Ru-N ₆	2.038(3)
N ₁ -Ru-N ₂₁	80.33(6)	N ₅ -Ru-N ₁	87.53(9)
N ₁ -Ru-N ₂₂	98.06(7)	N ₅ -Ru-N ₂	90.84(10)
N ₁ -Ru-N ₁₁	104.62(7)	N ₅ -Ru-N ₄	97.90(10)
N ₁ -Ru-N ₃₁	91.09(7)	N ₅ -Ru-N ₆	89.03(10)
N ₃₁ -Ru-N ₂₁	106.82(7)	N ₆ -Ru-N ₁	95.36(10)
N ₃₁ -Ru-N ₁₂	87.65(7)	N ₆ -Ru-N ₃	92.60(10)
N ₃₁ -Ru-N ₁₁	81.77(7)	N ₆ -Ru-N ₄	91.19(10)
N ₂₁ -Ru-N ₂₂	77.16(6)	N ₁ -Ru-N ₂	78.95(9)
N ₁₁ -Ru-N ₁₂	79.01(7)	N ₃ -Ru-N ₄	78.39(10)

^a Estimated standard deviations in least significant digits are given in parentheses.

5.4 Hz), 8.41 (d, 1H, $J = 8.1$ Hz), 8.39 (d, 1H, $J = 7.8$ Hz), 8.31 (d, 2H, $J = 7.8$ Hz), 8.24 (dt, 1H, $J = 1.5, 7.8, 7.8$ Hz), 8.16 (dt, 1H, $J = 1.5, 7.8, 7.8$ Hz), 7.95 (ddt, 2H, $J = 1.5, 2.1, 8.1, 8.1$ Hz), 7.90–7.77 (m, 2H), 7.77–7.62 (m, 3H), 7.39–7.29 (m, 3H), 7.26 (ddd, 1H, $J = 1.5, 5.7, 7.2$ Hz), 2.31 (s, 3H). ESI-MS (m/z , acetone) 679, {[**3**][PF₆]⁺}; 641, {[Ru(bpy)₂(CH₃CN)][PF₆]⁺}; 512, {Ru(bpy)₂(py)][F]⁺. UV-vis (CH₃CN, λ_{max} , nm (ϵ , M⁻¹cm⁻¹)): 436 nm (8500).

[Ru(L5pyr)(CH₃CN)][PF₆]₂ (1**)[PF₆]₂.** A solution of the ligand L5pyr (355 mg, 0.801 mmol) and RuCl₂(dmsO)₄ (417 mg, 0.861 mg) in 750 mL of absolute ethanol was refluxed in the dark for 15 h. The solution was concentrated in vacuo and the crude residue dissolved in acetonitrile to exchange the chloro ligand with an acetonitrile molecule. The mixture was stirred for 30 min, concentrated in vacuo, and the resulting residue was dissolved in water (a minimum volume of ethanol is sometimes required for total solubilization). A large excess of NH₄PF₆ (1.3 g, 8.0 mmol) was added, and evaporation of ethanol resulted in the precipitation of the complex. The precipitate was filtered, washed with water (3 times), dissolved in a minimum volume of acetone, and precipitated once again by the addition of the solution in a large volume of ether. Filtration afforded the crude complex as a dark-red crystalline powder. Crystallization by slow diffusion of a 1:1 mixture of ether-CHCl₃ in a solution of the complex in acetone, and subsequent drying in vacuo gave the pure complex (503 mg; 72%). Single crystals suitable for X-ray analysis were obtained by slow diffusion of CHCl₃ in a solution of the complex in acetonitrile. Pertinent crystallographic data are summarized in Table 1: Triclinic, $P\bar{1}$, $a = 11.5616 \pm 0.0005$, $b = 12.2521 \pm 0.0007$, $c = 13.1504 \pm 0.0008$ Å; $\alpha = 83.182(1)^\circ$, $\beta = 81.136(1)^\circ$, $\gamma = 85.510(1)^\circ$; $V = 1824.1 \pm 0.2$ Å³; $Z = 2$; $R = 0.0654$. ¹H NMR (300 MHz, acetone-*d*₆ (ppm)) 8.71 (d, 1H, $J = 7.8$ Hz), 8.64 (d, 1H, $J = 8.1$ Hz), 8.42 (d, 1H, $J = 8.1$ Hz), 8.38 (dd, 1H, $J = 1.2, 8.1$ Hz), 8.36 (t, 1H, $J = 7.8$ Hz), 8.21 (t, 1H, $J = 7.8$ Hz), 8.22 (d, 1H, $J = 6.0$

Hz), 8.10–7.98 (m, 2H), 7.97–7.87 (m, 2H), 7.85 (dd, 1H, $J = 0.6, 5.7$ Hz), 7.52 (d, 1H, $J = 7.5$ Hz), 7.34 (ddd, 2H, $J = 1.2, 6.0, 6.9$ Hz), 7.09 (d, 2H, $J = 7.8$ Hz), 4.70 (ddd, 1H, $J = 7.8, 11.7, 13.8$ Hz), 4.10–3.75 (m, 4H), 3.75–3.62 (m, 1H), 3.62–3.50 (m, 1H), 3.50–3.35 (m, 1H), 2.44 (s, 3H).

ESI-MS (m/z) 580, {RuL5pyrCl}⁺; 564, {RuL5pyrF}⁺; 292, {RuL5pyr(CH₃CN)}²⁺; 273, {RuL5pyr}²⁺. UV-vis (CH₃CN, λ_{max} , nm (ϵ , M⁻¹cm⁻¹)): 446 nm (7500).

Microanalysis for Ru(L5pyr)(CH₃CN)(PF₆)₂: calculated for C₃₁H₂₈N₆P₂F₁₂Ru: C%, 42.55, H%, 3.20, N%, 9.60, P%, 7.08 Ru%, 11.65. Found: C%, 42.43, H%, 3.32, N%, 8.93, P%, 6.63 Ru%, 11.4.

Standard Conditions for Sulfoxidation. To an acetone solution of catalyst (1 mM) was added 600 equiv of the sulfide, and the reaction was initiated by the addition of 15 equiv of H₂O₂. The reaction was monitored by GC from the amount of sulfoxide formed using benzophenone as an internal standard.

Standard Conditions for Epoxidation. To a dichloromethane solution of catalyst (0.6 mM) was added 50 equiv of the alkene, and the reaction was initiated by the addition of 125 equiv of PhI(OAc)₂. The reaction was monitored by GC from the amount of epoxide formed using benzophenone as an internal standard. The inhibition experiments by the acetate anion or cyclooctene oxide used similar conditions but in the presence of 15 equivalents of acetate or 30 equivalents of epoxide respectively.

Cyclovoltametric Experiments. The final solution issued from the sulfoxidation reaction by H₂O₂ catalyzed by complex **1** under standard conditions was evaporated, and the solid residue was washed with diethylether then dried under vacuum. The final solid was dissolved into an acetone solution containing 0.1 M of TBAP. The same method was performed for the epoxidation reaction.

Results

Synthesis of the Pentacoordinate Ligand L5pyr. The starting material 6-methyl-2,2'-bipyridine was synthesized by modifying reported procedures⁶ and was subsequently condensed, after deprotonation with LDA, onto 0.5 equiv of 2,6-bis(chloromethyl)pyridine into anhydrous ether at 0 °C (Scheme 1).¹¹ After purification by chromatography on neutral alumina, the pure ligand L5pyr was obtained in 54% yield.

Synthesis of **1 and **3**.** Refluxing a diluted ethanolic mixture of ligand L5pyr and RuCl₂(dmsO)₄ for 15 h yielded the complex [Ru(L5pyr)Cl]⁺. After concentration of the reaction mixture in vacuo, the substitution of the remaining chloro ligand by an acetonitrile one was easily and quantitatively achieved by solubilization of the crude residue in acetonitrile. Anion metathesis and subsequent crystallization by slow diffusion of a 1:1 ether-CHCl₃ mixture into a solution of the resulting complex as [**1**][PF₆]₂ in acetone afforded the pure complex in good yield (72%) and as a unique stereoisomer. The structure of **1** was determined by X-ray analysis from single crystals obtained by slow diffusion of chloroform in an acetonitrile solution of **1**.

3 was efficiently synthesized in two steps (85% yield) from [Ru(bpy)₂(py)Cl][PF₆]⁺ via the formation of the aquo complex [Ru(bpy)₂(py)(H₂O)][PF₆]₂ obtained by substitution of the chloro ligand by a water molecule and a subsequent fast and quantitative displacement of the latter by an acetonitrile

(11) Pomeranc, D.; Heitz, V.; Chambron, J. C.; Sauvage, J.-P. *J. Am. Chem. Soc.* **2001**, *123*, 12215.

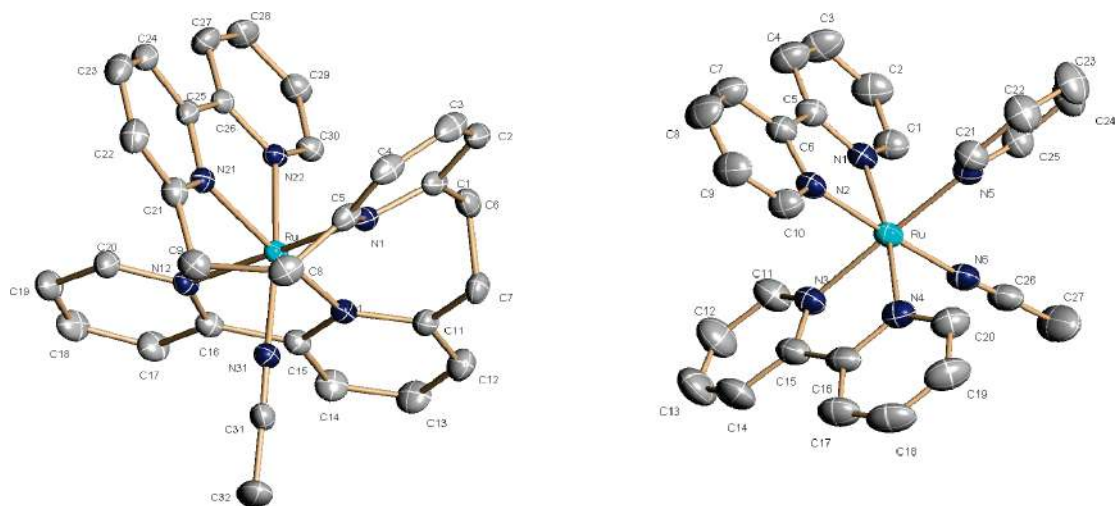


Figure 1. ORTEP views of the structures of **1** (left) and **3** (right). Hydrogen atoms have been omitted for clarity.

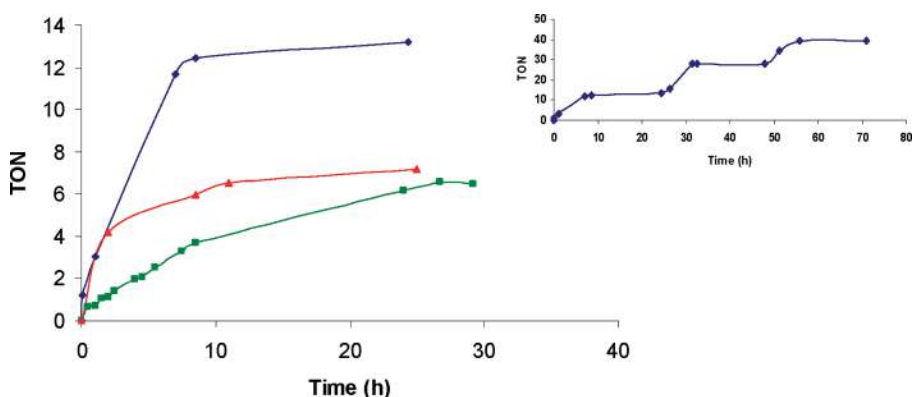


Figure 2. Catalytic oxidation of methylphenylsulfide (600 mM) to the corresponding sulfoxide using **1** (◆), **2** (■), and **3** (▲) as the catalyst (1 mM) and H₂O₂ (15 equiv) as the oxidant in acetone. Inset: the reaction catalyzed by **1** is monitored through the addition of three portions of hydrogen peroxide (15 equiv each).

one. This procedure was different from the one reported by Nagao et al.¹² **3** was then characterized by mass analysis and by ¹H NMR spectroscopy. Single crystals, suitable for X-ray analysis, were obtained by slow diffusion of ether into a solution of the complex in acetone. The X-ray structures of **1** and **3** are shown in Figure 1. Selected bond lengths and angles are given in Table 1. Similar values to those reported previously were observed for **3**.¹² As it can be seen, **1** and **3** are structurally highly similar, showing a distorted octahedral environment with the acetonitrile ligand in the cis position relative to the pyridine for **3** and to the pyridinyl moiety for **1**. However, two slight differences are worth being noted. First, to the exception of the Ru–N bonds trans to the pyridine ligand (or pyridinyl moiety for **1**), all of the Ru–N bond lengths in **1** are significantly longer than those in **3**. Second, whereas nearly all the N_{py}–Ru–N_{bp}y angles are close to 90° ± 5° in **3**, most of them in **1** are far from the ones expected for a pure octahedron geometry, reflecting the structural constraints caused by the ethylenic linkers (i.e., for **1**, N₁–Ru–N₂₁: 80°33; N₁–Ru–N₁₁: 104°62; N₃₁–Ru–N₂₁: 106°82).

Oxidation of Methylphenylsulfide by Hydrogen Peroxide. The catalytic properties of the ruthenium complexes were first evaluated during the oxidation of methylphenylsulfide as a probe substrate by hydrogen peroxide under standard conditions (catalyst: H₂O₂: substrate; 1:15:600 mM ratio, room temperature). Care was taken to avoid light exposure. In all of the experiments described below, only the corresponding sulfoxide was detected, and no evidence for the formation of the sulfone could be obtained. Furthermore, no oxidation products could be detected either in the absence of a ruthenium complex or when the reaction was performed in air in the presence of the catalyst. The results shown in Figure 2, in which **1**, **2**, and **3** are compared, clearly demonstrated that: (i) the coordination of a fifth pyridine (for **3**) or pyridinyl moiety (for **1**) greatly accelerated the sulfoxidation reaction, and (ii) **1** bearing the pentadentate ligand L5pyr proved to be the most efficient catalyst. In particular, reaction yields (based on H₂O₂) and TON were larger with **1** (about 90%, 13–14 catalytic cycles in 9 h) than those obtained with **3** (45% yield, 7 TON in about 12 h) and with **2** (about 40% yield, 6 TON after 24 h) (Table 2).

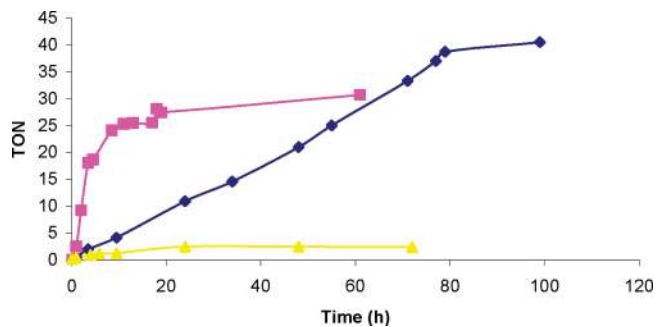
A further interesting property of **1** and **3** resides in their great stability. Indeed, as shown in the inset of Figure 2 in the case of **1**, the same rates and yields were obtained after

(12) Nagao, H.; Hirano, T.; Tsuboya, N.; Shiota, S.; Mukaida, M.; Woi, T.; Yamasaki, M. *Inorg. Chem.* **2002**, *41*, 6267.

Table 2. Catalytic oxidation of various substrates with catalysts **1**, **2** and **3**

catalyst	substrate	yield (%)	TON	TOF ^c (TON·h ⁻¹)
1	methylphenylsulfide ^a	90%	14	1.5
	cyclooctene ^b	80%	40	0.5
	<i>trans</i> - β -methylstyrene	74%	37	3.7
2	methylphenylsulfide ^a	40%	6	0.25
	cyclooctene ^b	<5%	<2	<0.1
3	methylphenylsulfide ^a	45%	7	0.6
	cyclooctene ^b	54%	27	1.35

^a a-catalyst/H₂O₂/substrate 1:15:600 mM ratio in acetone. ^b b-catalyst/PhI(OAc)₂/substrate 0.6:75:30 mM ratio in dichloromethane. ^c c-catalyst/PhI(OAc)₂/substrate 0.6:30:600 mM.

**Figure 3.** Catalytic oxidation of cyclooctene (50 equiv) using **1** (◆), **2** (■), and **3** (▲) as the catalyst (0.6 mM) and PhI(OAc)₂ (125 equiv) as the oxidant in dichloromethane.

the second and the third runs, showing that the catalyst was not altered under the reaction conditions. This was also true using **3** as a catalyst (data not shown). In contrast, **2** was completely inactivated after a first reaction run. This clearly established the importance of the fifth pyridine ligand for stability of the catalyst. Finally, the lower TONs observed for catalysts **2** and **3** may be the result of a catalytic decomposition of the oxidant by these catalysts, even if no evidence of the dismutation reaction was observed during the reaction time. However, as far as **2** is concerned, it seems obvious that its low activity was mainly due to its progressive inactivation rather than its ability to decompose hydrogen peroxide.

Oxidation of Cyclooctene by [Bis(acetoxy)-iodo]benzene. The second reaction probe was cyclooctene epoxidation by [bis(acetoxy)-iodo]benzene, PhI(OAc)₂. The reaction mixture contained the ruthenium complex (0.6 mM), PhI(OAc)₂, and cyclooctene in a 1:125:50 ratio in dichloromethane at room temperature. In this case, the excess of oxidant was employed for high conversion of the substrate. Under those conditions, only the corresponding epoxide was produced. In the absence of the catalyst, less than 1% epoxide was generated after 2 days of reaction. Hydrogen peroxide proved inefficient because, in the best case, even at 45 °C, the yield based on the substrate was about 15%.

As shown in Figure 3 and Table 2, **1** and **3** proved to be greatly superior to **2**, thus confirming the stimulating effect of the fifth pyridine ligand. With **3** as a catalyst, more than 50% of the substrate was converted to the corresponding epoxide (>27 TON), as compared to less than 5% with **2** (<2 TON). **1** again provided the highest yield because more than 80% of the substrate was converted into the epoxide during one catalytic run (>40 TON), however, at smaller

rates the maximum conversion was reached after only 10 h for **3**, whereas 80 h were required for **1** (Figure 3). We also showed that the PhI(OAc)₂-**1** system was able to oxidize other olefins such as *trans*- β -methylstyrene into the corresponding *trans*-epoxide (74% yield, 37 TON after 10 h; **1**/PhI(OAc)₂/substrate, 1:50:1000) in dichloromethane at room temperature without formation of benzaldehyde.

The great stability of the catalyst **1** was observed during a second and third catalytic run. Indeed, addition of a second and then a third batch of substrate and oxidant results in similar yields and rates. This indicates the possibility of making at least several hundreds of turnovers with this system. In contrast, after the first run, addition of a second aliquot of the oxidant to the reaction mixture containing the catalyst **3** did not result in further oxidation of cyclooctene. This can be attributed to the total inactivation of **3** after the first 10 h (Figure 3). However, as it was observed by UV-vis, ¹H NMR, cyclic voltammetry, and ESI-MS, that **3** recovered from the reaction mixture proved to be unchanged. Furthermore, the reactivity of the extracted **3** reengaged for a second time in the oxidation of cyclooctene was found almost unchanged. These results highly suggested that **3** was inactivated by a product of the reaction, namely, the acetate anion issued from the oxidant. Indeed: (i) the addition of 15 equiv of acetate anion in the reaction mixture inhibited the epoxidation by 80%; (ii) a **3**-acetate complex was observed both by UV-vis spectroscopy associated with a slight shift of the 450 and 550 nm transitions (part B of Figure 4), and by ESI-MS analysis with a fragment at *m/z* = 473 assigned to the [Ru(bpy)₂(OAc)]⁺ species; (iii) no inactivation of **3** was observed during oxidation of cyclooctene by PhIO instead of PhI(OAc)₂, even if a lower rate was observed as a consequence of the low solubility of this oxidant.

Self-Oxidation of 1. **1** was monitored by UV-vis spectroscopy during the reaction with H₂O₂ (15 equiv) in the presence of methylphenylsulfide in excess. Addition of H₂O₂ resulted in the immediate conversion of the original spectrum containing a CT band at 446 nm into a new spectrum displaying absorption bands characterized by two shoulders around 360 and 440 nm (part A of Figure 4). These features were similar to those previously reported for [Ru(III)(bpy)(py)(OH)]²⁺.^{3,13} This spectrum as well as the spectroscopic features described below support the conclusion that the complex has been converted into a ruthenium(III) species, **1'**.

The oxidation of ruthenium(II) to ruthenium(III) was also confirmed by ¹H NMR of the new complex, in acetone-*d*₆, which did not show any diamagnetic resonances but broad paramagnetic resonances at 20, 18, 12 and 11 ppm. Furthermore the 4 K EPR spectrum was consistent with the presence of a paramagnetic *S* = 1/2 species (inset Figure 5) accounting for more than 50% of the total ruthenium. In addition, the following data demonstrated a change in the coordination sphere of the ruthenium center. First, whereas the cyclic voltammogram (CV) of **1** displayed a single redox active process at 1.15 V versus Ag/AgCl assigned to the ruthenium(II)/ruthenium(III) couple, that of the new **1'**, recorded

(13) Stultz, L. K.; Binstead, R. A.; Reynolds, M. S.; Meyer, T. J. *J. Am. Chem. Soc.* **1995**, *117*, 2520.

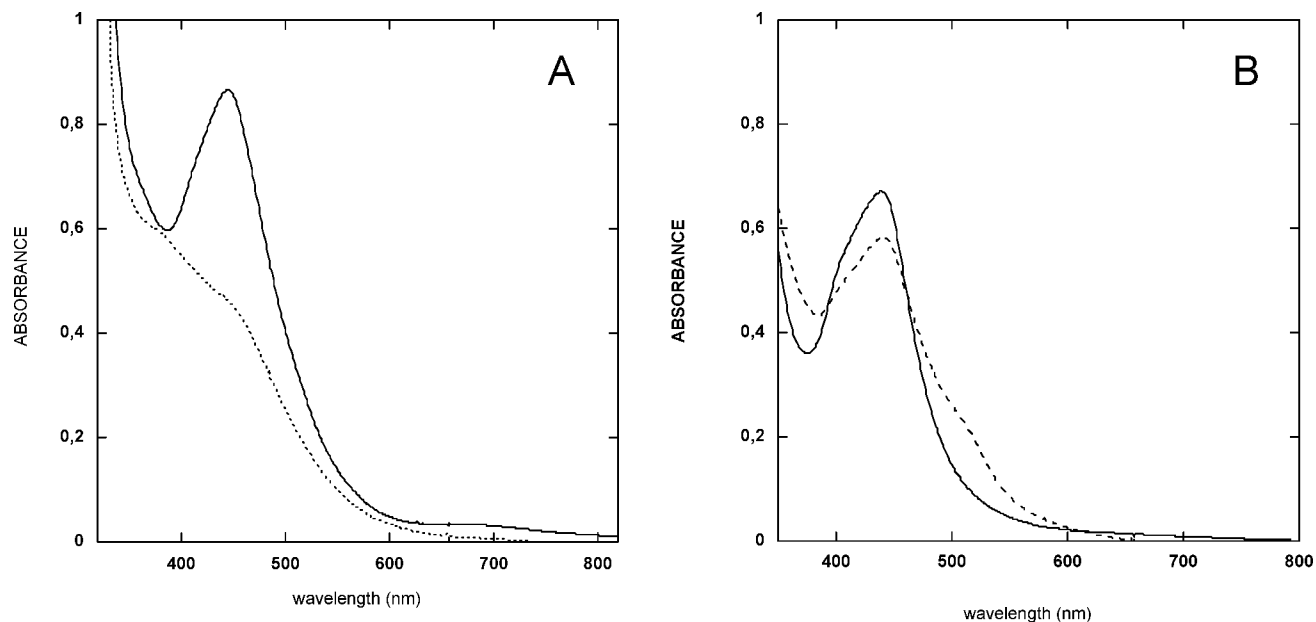


Figure 4. (A) UV-vis spectrum of **1** (1.2 mM)/H₂O₂/methylphenylsulfide reaction mixture in dichloromethane/**1** before addition of H₂O₂ (solid line); 6 h after addition of the oxidant (dashed line). (B) UV-vis spectrum of **3** (0.7 mM)/PhI(OAc)/cyclooctene in dichloromethane/**3** before addition of PhI(OAc)₂ (solid line); 80 h after addition of the oxidant (dashed line).

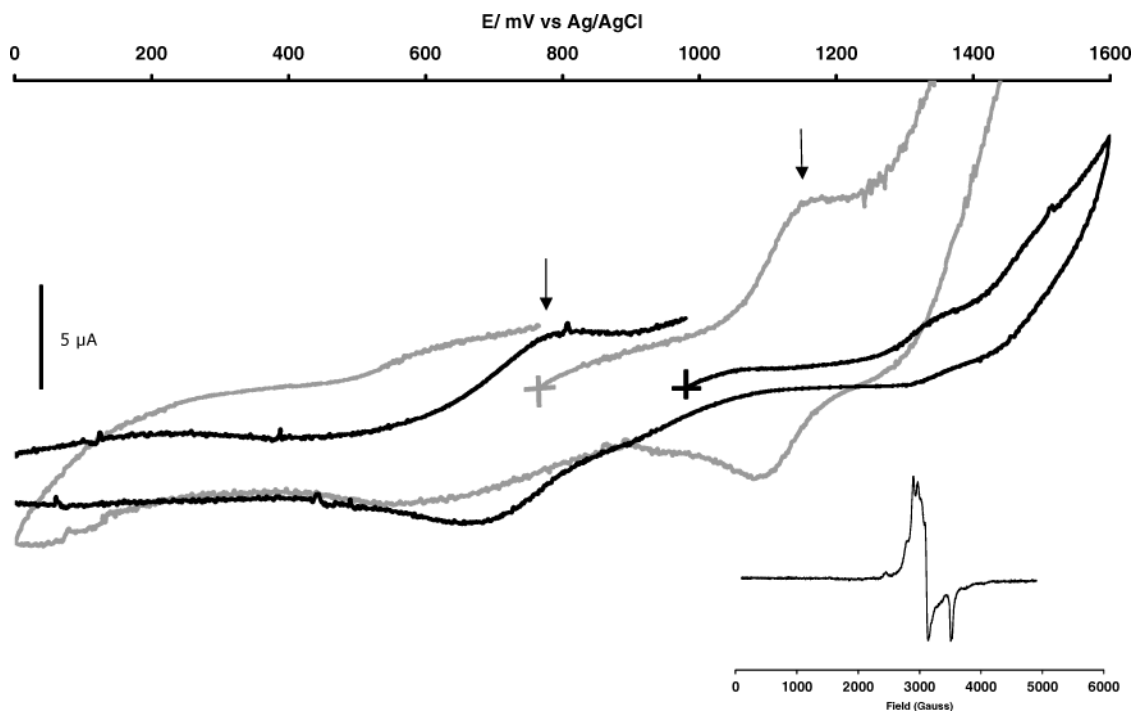


Figure 5. Cyclic voltammograms of **1** (1 mM) in acetone on a platinum electrode at 100 mV s⁻¹ before H₂O₂ addition (gray) and of the resulting **1'** extracted from the reaction mixture (black). Inset: EPR spectrum of the final solution in acetone; experimental conditions: microwave power 200 μW, receiver Gain 8 10⁴; microwave frequency 9.446 GHz, Modulation amplitude 10 Gauss, temperature 15 K.

after extraction from the reaction catalytic mixture or after hydrogen peroxide treatment, displayed a new redox process at 0.740 V (Figure 5). The decrease of the redox potential of the ruthenium(II)/ruthenium(III) couple indicates that ruthenium is coordinated by a more electron-rich environment, thus causing a stabilization of the ruthenium(III) state. Second, the ESI-MS spectrum of the new complex revealed fragments at *m/z* 280, 289, and 705 assigned to [Ru(III)(L5pyr)-H + O]²⁺ and [Ru(III)(L5pyr)(OH₂)-H + O]²⁺ and [Ru(III)-(L5pyr)-H + O + (PF₆)]⁺ respectively (Figure 6), as supported

by the agreement between the isotopic pattern of each fragment and the theoretical one (Supporting Information). All of these data are consistent with a monohydroxylation of the ligand L5pyr. Because no hydroxylation of **3** could be observed, we thus propose that the ligand L5pyr has been hydroxylated at one of the ethylidene moieties and that the introduced oxygen coordinates the ruthenium center, allowing a stabilization of the ruthenium(III) state (Scheme 2). All of our efforts to isolate and resolve a 3D structure of **1'** were unsuccessful. However, this conclusion is supported by a similar observation reported

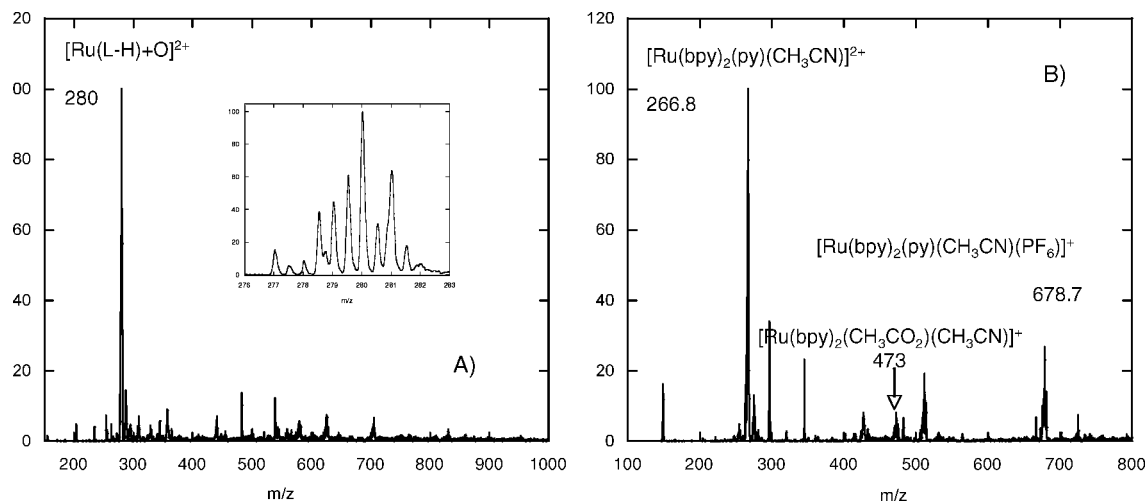
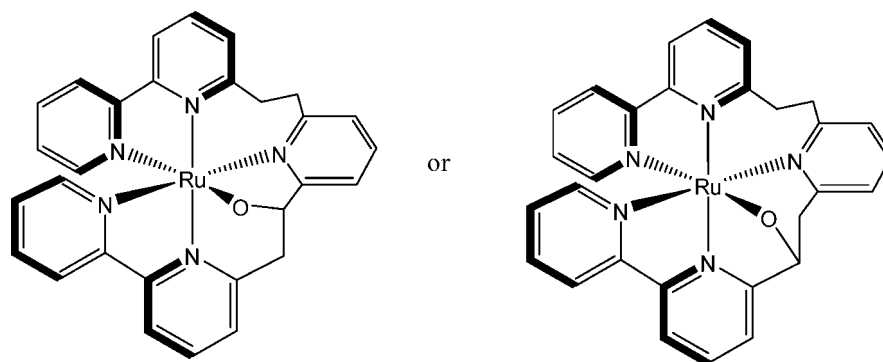


Figure 6. (A) ESI-MS spectra of **1** with H_2O_2 after 24 h reaction; inset: fragment at m/z 280. See Supporting Information for comparison with theoretical spectrum. (B) ESI-MS spectrum of **3** with $\text{PhI}(\text{OAc})_2$ after 80 h reaction. The arrow indicates the fragment of the acetato adduct.

Scheme 2. Proposed Structures for **1'**



by Che and co-workers with a $[\text{Ru}(\text{III})(\text{tepa})(\text{H}_2\text{O})(\text{OH})]^{2+}$ complex (tepa = tris(2-(2-pyridyl)ethyl)amine).¹⁴ They isolated and characterized a stable $[\text{Ru}(\text{III})(\text{N}_4\text{O})(\text{H}_2\text{O})]^{2+}$ complex resulting from the hydroxylation of the tetradentate ligand at an activated benzylic C–H bond by the ruthenium(III) metal and H_2O_2 or O_2/Ag^+ .

It is worth noting that the same transformation of our complex was observed with $\text{PhI}(\text{OAc})_2$ (125 equiv) as the oxidant (data not shown). In addition, in both cases, no noticeable induction period corresponding to the oxidation of the ligand has been observed.

Discussion

Surprisingly, very little has been done to improve the activity and the stability of well-studied bis-diimine-ruthenium catalysts. Here, we report the interesting observation that an additional nitrogen-based ligand such as pyridine greatly activates the Ru^{2+} center, resulting in larger reaction rates, larger yields, and larger stabilities during oxidation reactions using H_2O_2 or $\text{PhI}(\text{OAc})_2$ as the oxidant. This is clearly shown from the comparison of **2** and **3** during sulfoxidation and epoxidation. However, when this additional pyridine is a part of a pentadentate ligand, such as L5pyr, a different chemistry took place (Figures 2 and 3).

The oxidizing properties of the $[\text{Ru}(\text{IV})(\text{bpy})_2(\text{py})(\text{O})]^{2+}$ complex have been extensively studied, and it is proven that

such species are involved in oxo-transfer reactions catalyzed by **3**.¹⁵ The stimulating effect of the fifth pyridine ligand might be due to the resulting increased electron density at the ruthenium center, thus facilitating the formation of the high-valent ruthenium(IV) complex. It is tempting to suggest, on the basis of the structural similarities, that this is also occurring in the very initial phase of the reactions catalyzed by **1**. However, in that case, the Ru^{IV} -oxo intermediate preferentially reacts with one proximal methylene group of the L5pyr ligand. This results in an immediate monohydroxylation of the ligand, as shown by mass spectrometry, and formation of an alkoxo-Ru bond, stabilizing a ruthenium(III) center, under the oxidizing conditions of the reaction, as shown by UV–vis and EPR spectroscopy. Thus, **1** is converted into **1'** with a N_3O coordination almost instantaneously, and the latter is proposed to be the active catalyst, with no further oxidation of the ligand. The mechanism of the reactions catalyzed by **1'** is intriguing because ruthenium is now hexacoordinated, and activation of the oxidant would need liberation of at least one coordination site. The fact that **1** and **3** have significantly different properties (below) suggests that the alkoxo–Ru bond is retained during catalysis

(14) Che, C. M.; Yam, V. W.-W.; Mak, T. C. W. *J. Am. Chem. Soc.* **1990**, *112*, 2284.

(15) Meyer, T. J.; Huynh, M. H. V. *Inorg. Chem.* **2003**, *42*, 8140.

and, as a consequence, the labile ligand could be the pyridine moiety. In such a case, the presence of the pyridine moiety is only required to allow the hydroxylation of the ligand.

It is a rather unexpected finding that the hydroxylation of the pentadentate ligand does not lead to an inactivation of the catalyst (note that in the case of the epoxidation reaction, rates are nevertheless smaller, compare **1** and **3**). In addition, this modification seems to afford a better resistance to the acetate anion inhibitor. It is also possible that the first monohydroxylation prevents the catalyst from further oxidative degradation. Self-oxidation of the organic ligand is a frequent problem encountered in catalytic oxidation systems based on coordination complexes. This important issue has been addressed through the design of oxygen-resistant ligands such as, for example, perhalogenated metalloporphyrins¹⁶ or tetraamido macrocyclic ligands.¹⁷ There are several interesting reports in the literature of studies aimed at characterizing

the oxidation reactions occurring at the level of the ligand in iron-, copper-, or nickel-based systems.^{18–20} Some of these reactions lead to degradation and decomposition of the organic component of the complex. More interestingly, in some cases the reaction consists of the selective introduction into the ligand of an oxygen atom, which subsequently gets coordinated to the metal center. To our knowledge, in all cases, these modifications result in complete inactivation of the catalyst. In this article, we report a unique case in which the selective oxidation of the ligand converts a complex into an active, remarkably stable, catalyst.

-
- (16) (a) Dolphin, D.; Traylor, T. G.; Xie, L. Y. *Acc. Chem. Res.* **1997**, *30*, 251. (b) Meunier, B. *Chem. Rev.* **1992**, *92*, 1411.
(17) Collins, T. J. *Acc. Chem. Res.* **2002**, *35*, 782.

-
- (18) (a) Lewis, E. A.; Tolman, W. B. *Chem. Rev.* **2004**, *104*, 1047. (b) Itoh, S. In *Comprehensive Coordination Chemistry II*; Que, L., Jr., Tolman, W. B., Eds; Elsevier: Amsterdam, 2004; Vol. 8, pp 369–393. (c) Jensen, M. P.; Lange, S. J.; Mehn, M.P.; Que, E. L.; Que, L. *J. Am. Chem. Soc.* **2003**, *125*, 2113.
(19) (b) Mekmouche, Y.; Ménage, S.; Duboc-Toia, C.; Fontecave, M.; Galey, J.-B.; Lebrun, C.; Pécaut, J. *Angew. Chem.* **2001**, *40*, 949.
(20) Maiti, D. N.; Lucas, H. P.; Sarjeant, A. A.; Karlin, K. D. *J. Am. Chem. Soc.* **2007**, *129*, 6998.